International Journal for Multiscale Computational Engineering, 7(6)577–594(2009)

Inverse Shallow-Water Flow Modeling Using Model Reduction

Muhammad Umer Altaf, Arnold W. Heemink, & Martin Verlaan*

Delft University of Technology, Mekelweg 4, 2628 CD, Delft, The Netherlands

ABSTRACT

The idea presented in this paper is variational data assimilation based on model reduction using proper orthogonal decomposition. An ensemble of forward model simulations is used to determine the approximation of the covariance matrix of the model variability, and only the dominant eigenvectors of this matrix are used to define a model subspace. An approximate linear reduced model is obtained by projecting the original model onto this reduced subspace. Compared to the classical variational method, the adjoint of the tangent linear model is replaced by the adjoint of a linear reduced forward model. Thus, it does not require the implementation of the adjoint of the tangent linear model. The minimization process is carried out in reduced subspace and hence reduces the computational cost. Twin experiments using an operational storm surge prediction model in the Netherlands, the Dutch Continental Shelf Model are performed to estimate the water depth, with the findings that the approach with relatively little computational cost and without the burden of implementation of the adjoint model can be used in variational data assimilation.

KEYWORDS

inverse modeling, proper orthogonal decomposition, shallow-water tides

*Address all correspondence to m.u.altaf@ewi.tudelft.nl

1. INTRODUCTION

Variational data assimilation has often been used for model calibration (e.g., [1–4]). The method aims at adjusting a number of unknown parameters on the basis of given data. One first defines a scalar function, which, for any model solution over the assimilation interval, measures the "distance" or "misfit" between that solution and the available observations. The so-called objective (cost) function will typically be a sum of squared differences between the observations and the corresponding model values. One will then look for the model solution that minimizes the objective function. To obtain a computationally efficient procedure, this objective function is minimized with a gradient-based algorithm where the gradient is determined by solving the adjoint problem. Usually, variational data assimilation requires the implementation of an adjoint model. Research has recently been carried out on automatic generation of computer code for the adjoint, and adjoint compilers have now become available (see [5]). Even with the use of these adjoint compilers, this is a laborious programming effort that hampers new applications of the method.

In the last several years, the study of many complex systems has taken strong advantage of the development of mathematical methods coming from the theory of nonlinear dynamical systems. Proper orthogonal decomposition (POD) is a model reduction method considered as an application of the SVD to the approximation of general dynamical systems [6]. POD can be the technique leading to useful low-dimensional ordinary differential equation approximations of partial differential equations models, allowing one to take full advantage of dynamical systems theory. The method was originally developed by Karl Pearson (see [7]) and has application in many fields, such as image processing, signal processing, data compression, oceanography, chemical engineering, and fluid mechanics (see e.g., [8–11]). For a detailed description on POD scope and research, see [12].

Another application of POD in operational occeanography and weather forcasting is four-dimensional variational data assimilation (4DVAR), which is based on optimal control theory [13]. POD has recently been applied succesfully in 4DVAR (e.g., [14–17]). Previous experiences show that the POD is valuable in parameter estimation (e.g., [18]), especially the recent work by [19] shows that a POD-based model reduction technique can be successfully applied for inverse modeling of 3D groundwater flow.

In the POD model reduced approach presented here, an ensemble of snapshot vectors of forward model simulations is used to determine an approximation of the covariance matrix of the model variability and a small number of leading eigenvectors of this matrix are used to define a model subspace. By projecting the original model onto this subspace, an approximate linear reduced model is obtained. Once the reduced model is available, its adjoint can be implemented easily and the minimizing problem is solved completely in reduced space with very low computational cost. If necessary, this process of minimization is repeated several times by generating a new set of snapshots (ensemble), which is closer to the new estimated parameters.

Compared to the classical variational method, the adjoint of the tangent linear model is replaced by the adjoint of a linear reduced forward model. While the adjoint of the tangent linear approximation of the original model produces the exact local gradient, the reduced-order approach is based on a statistically linearized model and hence produces an averaged gradient. As a result the model reduced approach can be less sensitive for local minima for certain applications [20].

The main motivation for the present work is inspired by the recent work done in reduced-order modeling by [14, 20]. These methods are based on deriving approximate low-order data assimilation system in the context of the incremental 4DVAR procedure for parameter and state estimation, respectively. In the present work, we consider *(i)* a new application of reduced-order calibration approach. The method has been used for a model based on shallow water equations, which is different in behavior from one used by [20]. We also consider *(ii)* using extended time horizon for parameter estimation. The generation of an ensemble involves running the forward model several times. The computational cost of the method is dominated by the generation of this ensemble. In this study, it is found that if the dynamics of the system does not change significantly then a smaller simulation period can be chosen to generate an ensemble of forward model simulations for an optimization problem over a larger period.

A shallow-water model of the Continental Shelf, the Dutch Continental Shelf Model (DCSM), is used in The Netherlands to forecast the storm surges in the North Sea. Accurate predictions of storm surges are of vital importance to The Netherlands. The decision whether or not to close the storm surge barriers is based on these predictions. A number of twin experiments are performed with DCSM to evaluate the performance of the proposed approach. This allows us to evaluate the results by comparing them to the truth. The paper is organized as follows. Section 2 explains classical inverse modeling methods. A procedure required for the construction of POD projection-based reduced method is described in Section 3. In Section 4 a proposed algorithm of calibration is described. Section 5 contains experiments with the operational model for storm surge prediction, the DCSM, to estimate the water depth. The paper concludes in Section 6 by disscussing the results.

2. INVERSE MODELING

Consider the data assimilation problem as general nonlinear dynamical system. The discrete system equation for the state vectors $\mathbf{x}(t_i) \in \Re^n$ is given by

$$\mathbf{x}(t_{i+1}) = M_i[\mathbf{x}(t_i), \gamma] \tag{1}$$

where M_i is a nonlinear and deterministic dynamics operator that includes inputs and propogates the state from time t_i to time t_{i+1} and γ is the vector of uncertain parameters that need to be determined. Suppose now that we have imperfect observations $\mathbf{y}(t_i) \in \Re^q$ of the dynamical system (1), which are related to model state at time t_i through

$$\mathbf{y}(t_i) = H\mathbf{x}(t_i) + \eta(t_i) \tag{2}$$

with $H : \Re^n \rightarrow \Re^q$ is a linear observation operator that maps the model fields on observation space and $\eta(t_i)$ is an unbiased, random Gaussian error vector with covariance matrix R_i.

The idea of parameter estimation is to identify the values of uncertain model parameters γ. We assume that the difference between data and simulation results is only due to measurement errors and incorrectly prescribed model parameters. A most commonly used measure that determines this difference is the weighted sum of squared residuals. The problem of estimation is then solved by directly minimizing the cost function J

$$\begin{aligned} J(\gamma) = \sum_{i=1}^{m} \{\mathbf{y}(t_i) - H[\mathbf{x}(t_i)]\}^T \\ \times R_i^{-1} \{\mathbf{y}(t_i) - H(\mathbf{x}(t_i))\} \end{aligned} \tag{3}$$

with respect to the parameters γ, satisfying the discrete nonlinear forecast model (1).

The minimization of the cost function (J) is often based on quasi-Newton methods. These methods require the computation of the gradient of the cost function. The gradient vector (∇J) gives information about the direction (positive or negative) and the size of adjustments for each individual parameter. The adjoint method [21] computes the exact gradient efficiently. The principle of the adjoint method is based on the systematic use of the chain rule of differentiation. Regardless of the number of parameters, the time required to compute the gradient using the adjoint technique is more or less identical and comparable to the computational time needed for a single simulation run of the nonlinear model (1). It requires one forward simulation with original the nonlinear model (1) and a second additional simulation backward in time with the adjoint model

$$\begin{aligned} \nu(t_i) = \left[\frac{\partial M_i}{\partial \mathbf{x}(t_i)}\right]^T \nu(t_{i+1}) - 2HR_i^{-1} \\ \times \{\mathbf{y}(t_i) - H[\mathbf{x}(t_i)]\} \end{aligned} \tag{4}$$

where $\nu(t_i)$ represents the solution of the adjoint model. The gradient ∇J of the cost function (J) with respect to each component $\gamma_k; k = \{1, \ldots, u\}$ of the uncertain parameters vector γ is given by

$$\nabla J_k = \sum_{i=1} - [\nu(t_{i+1})]^T \left\{\frac{\partial M_i[\mathbf{x}(t_i), \gamma]}{\partial \gamma_k}\right\} \tag{5}$$

The main hurdle in the use of the adjoint method is its implementation. Even with the use of adjoint compilers that have become available these days, this is a huge programming effort that hampers new applications of the method. Second, the adjoint equation needs to be integrated backward in time, and therefore, the states of the forward model have to be stored at each grid point for all time steps. The memory access will therefore be huge for large-scale problems.

3. REDUCED-ORDER MODELING

The problem of obtaining a lower-dimensional approximation to a high-dimensional system is known as model reduction. The methods used in this paper fall in the category of projection methods, in that they involve projecting the system equations onto a subspace of the original phase space.

3.1 Proper Orthogonal Decomposition

The proper orthogonal decomposition, also known as principle components analysis, has been widely used for a broad range of applications. POD analysis yields a set of empirical eigenfunctions, which describes the dominant behavior or dynamics of given problem. The eigenfunctions obtained from POD can efficiently display possible spatial localizations, even strongly time dependent. It can be classified as one that examines the linear relationship between variables with the aim of reducing the dimensionality of the problem.

The main idea is, given a set of data that lies in a vector space V, to find a subspace V_r of fixed dimension r, such that the error in the projection onto the subspace is minimized. We start by collecting the set of s snapshots of some physical process. Each sample of snapshots $\mathbf{x}_i$ that is defined on a set of n node $\mathbf{x}$ stands for an n-dimensional vector $\mathbf{x}_j$, i.e.,

$$\mathbf{x}_i = \{x_{1i}, x_{2i}, \cdots, x_{ni}\}'; \quad i \in \{1, 2, \cdots, s\} \tag{6}$$

The elements within a snapshot represent the signal for a specific location in the model, possibly for multiple quantities. Define the vector $\mathbf{x}_b$ of background state and correct each snapshot vector so that

$$\mathbf{e}_i = \mathbf{x}_i - \mathbf{x}^b \tag{7}$$

These corrected snapshots are arranged in matrix E, which denote the new ensemble. The covariance matrix Q can be constructed from the ensemble E of the snapshots by taking the outer product

$$Q = EE^t \tag{8}$$

The dimension n often exceeds 10^4; thus, a direct solution of eigenvalue problem is not often feasible. To shorten the calculation time necessary for solving the eigenvalue problem for this high-dimensional covariance matrix, we define a covariance matrix G as the inner product. In the method of snapshots [22], one then solves the $s \times s$ eigenvalue problem

$$G\mathbf{z}_i = E^t E\mathbf{z}_i = \lambda_i \mathbf{z}_i; \quad i \in \{1, 2, \cdots, s\} \tag{9}$$

with λ_i are the eigenvalues of the above eigenvalue problem. The eigenvectors z_i may be chosen to be orthonormal and the POD modes P are then given by

$$\mathbf{p}_i = \frac{\sqrt{\lambda_i}}{E\mathbf{z}_i} \tag{10}$$

A physical explanation of POD modes is that they maximize the average energy in the projection of data onto the subspace spanned by the modes. The eigenvalues λ_i provide a measure (ψ_i) for the relative energy associated with corresponding POD modes p_i

$$\psi_i = \frac{\lambda_i}{\sum_{l=1}^{s} \lambda_l}.100\%; \quad i = \{1, 2, \ldots, s\} \tag{11}$$

We collect p_r ($r < s$) modes such that $\psi_1 > \psi_2 > \cdots > \psi_r$ and they totally explain at least the required variance ψ^e

$$\psi^e = \sum_{l=1}^{r} \psi_l \tag{12}$$

4. INVERSE MODELING USING REDUCED MODEL

An approximate linear reduced model in variational data assimilation presented here is based on the principle of POD model reduction technique. An ensemble of snapshots vectors are generated from the original model. The reduced model operates on the space defined by the dominant eigenvectors of the generated ensemble.

4.1 Linearization and Reduced Basis

Linearization of nonlinear high-order model (12) with respect to estimate variable γ_k gives

$$\begin{aligned}\overline{\mathbf{x}}(t_{i+1}) &= M_i[\mathbf{x}^b(t_i), \gamma^b]\overline{\mathbf{x}}(t_i) \\ &+ \sum_{k=1} \frac{\partial M_i[\mathbf{x}^b(t_i), \gamma^b]}{\partial \gamma_k} \Delta\gamma_k\end{aligned} \tag{13}$$

with $\bar{\mathbf{x}}$ is linearized state and $\mathbf{x}^b$ is the background state for which the corresponding estimate variables γ^b are linearized. The partial derivatives $\partial M/\partial\gamma_k$ can be computed using perturbation with respect to estimate variable γ_k

$$\frac{\partial M_i}{\partial \gamma_k} \approx \frac{M_i[\mathbf{x}^b(t_i), \gamma_k^b + \Delta\gamma_k] - M_i[\mathbf{x}^b(t_i), \gamma_k^b]}{\Delta\gamma_k} \quad (14)$$

with $\Delta\gamma_k$ a the perturbation. We choose snapshot vectors $\mathbf{e}_i$ from these perturbations along estimate variable γ_k.

These snapshots are collected in matrix $E = \{\mathbf{e}_1, \ldots, \mathbf{e}_s\}$. We then simplify the eigenvalue problem as explained in Section 3.1 to obtain the POD basis (modes) $P = \{\mathbf{p}_1, \ldots, \mathbf{p}_r\}$ of r dominant eigenvectors. The total number of eigenmodes r in the basis P depends on the required accuracy of the reduced model.

4.2 Reduced Model Formulation

A model can be reduced if state $\hat{\mathbf{x}}(t_i)$ can be written as linear combination

$$\hat{\mathbf{x}}(t_{i+1}) = \mathbf{x}^b(t_{i+1}) + P\xi(t_{i+1}) \quad (15)$$

where $\hat{\mathbf{x}}$ is the approximate linearized state and ξ is a reduced time-varing state vector given by

$$\xi(t_{i+1}) = \widetilde{M}_i\xi(t_i) + \sum_{k=1} \frac{\partial \widetilde{M}_i}{\partial \gamma_k}\Delta\gamma_k \quad (16)$$

or in matrix form

$$\begin{pmatrix} \xi(t_{i+1}) \\ \Delta\gamma \end{pmatrix} = \begin{pmatrix} \widetilde{M}_i & \widetilde{M}_i^{\gamma} \\ 0 & I \end{pmatrix} \begin{pmatrix} \xi(t_i) \\ \Delta\gamma \end{pmatrix} \quad (17)$$

$\widetilde{M}_i$ and $\widetilde{M}_i^{\gamma}$ are simplified dynamics operators, which approximate the full Jacobians $\partial M_i/\partial x^b$ and $\partial M_i/\partial\gamma_k$, respectively.

$$\widetilde{M}_i = P^T \frac{\partial M_i}{\partial \mathbf{x}^b(t_i)} P \quad (18)$$

$$\widetilde{M}_i^{\gamma} = P^T \left(\frac{\partial M_i}{\partial \gamma_1}, \cdots, \frac{\partial M_i}{\partial \gamma_u} \right) \quad (19)$$

The Jacobian $\partial M_i/\partial \mathbf{x}^b$ is obtained by approximating the nonlinear dynamics operator M_i by linearizing it with respect to background state $\mathbf{x}^b$. Instead of computing this huge Jacobian by approximating the partial differential with finite difference by perturbing the nonlinear operator M_i in the direction of each node, we perturb, along the direction of POD modes only

$$\frac{\partial M_i}{\partial \mathbf{x}^b(t_i)} p_h = \frac{M_i[\mathbf{x}^b(t_i) + \varepsilon p_h, \gamma^b] - M_i[\mathbf{x}^b(t_i), \gamma^b]}{\varepsilon} \quad (20)$$

with ε be the size of the perturbation. The reduced dynamics operator $\widetilde{M}_i$ can now be computed by premultiplying the above formulae by P^T

$$\widetilde{M}_i = P^T \left[\frac{\partial M_i}{\partial \mathbf{x}^b(t_i)} p_1, \cdots, \frac{\partial M_i}{\partial \mathbf{x}^b(t_i)} p_r \right] \quad (21)$$

The dimension on which reduced model operates depends on the number of eigenmodes (r) selected in the POD basis and the number of estimate variables (u), i.e., $(r + u) \times (r + u)$.

4.3 Approximate Objective Function and Its Adjoint

The value of the approximate objective function $\hat{J}$ is obtained by correcting the observations $\mathbf{y}(t_i)$ for the background state $\mathbf{x}^b(t_i)$, which is mapped on the observational space through a mapping H and to the reduced model state $\xi(t_i)$, which is mapped on the observational space through mapping $\hat{H}$, with $\hat{H} = HP$

$$\begin{aligned} \hat{J}(\Delta\gamma) = &\sum_{i=1}^{m} \Big[\{\mathbf{y}(t_i) - H(\mathbf{x}^b(t_i))\} - \hat{H}\xi(t_i, \Delta\gamma) \Big]^T \\ &\times R_i^{-1} [\{\mathbf{y}(t_i) - H(\mathbf{x}^b(t_i))\} - \hat{H}\xi(t_i, \Delta\gamma)] \end{aligned} \quad (22)$$

Because the dimension of the reduced model is smaller than that of original model and reduced model has linear characteristics, it is easy to build an approximate adjoint model for the computation of gradient of the approximate objective function (22). The gradient of $\hat{J}$ with respect to estimate variable $\Delta\gamma$ is given by

$$\frac{\Delta\hat{J}}{\Delta\gamma} = \sum_i -[\hat{\mathbf{v}}(t_{i+1})]^T \frac{\partial \xi(t_{i+1})}{\partial \Delta\gamma} \quad (23)$$

where $\hat{\mathbf{v}}(t_{i+1})$ is the reduced adjoint state variable (see Appendix A). Once the gradient has been computed, the process of minimizing the approximate objective function $\hat{J}$ criterion has to be done along the direction of the gradient vector in the reduced space.

4.4 Procedural Flow with Reduced Model

In order to perform the whole parameter estimation process, the following steps are performed:

1. Outer Iteration:
   - Background initial parameters γ^b are used to generate an ensemble of forward model simulations.
   - A POD-reduced model and its adjoint model are established using this ensemble.
2. Inner Iteration:
   - Perform optimization iterations in reduced space to obtain the optimal solution of the approximate objective function $\hat{J}$.
   - After the minimization process the background initial parameters γ^b are updated and new set of initial parameters (γ^{up}) is obtained.

$$\gamma^{up} = \gamma^b + \Delta\gamma \tag{24}$$

3. Return to step 1 with new set of initial parameters until optimality condition is achieved.

4.5 Convergence Criterion for Inner and Outer Iterations

We have defined two criterions, both for the inner and outer iterations of the optimization process. We stop the present inner iteration and switch to a new outer iteration with a new set of parameters following the criterion μ, which is defined as

$$\mu = \sum_{k=1} \frac{\| \bigtriangledown \hat{J}_k^{\eta} \|}{\| \bigtriangledown \hat{J}_k^{b} \|} \leq \delta \tag{25}$$

with $\bigtriangledown \hat{J}_k^b$ is value of gradient for $\Delta\gamma_k$ at start of inner iteration, $\bigtriangledown \hat{J}_k^{\eta}$ is value of gradient for $\Delta\gamma_k$ after each inner iteration. The value of δ is chosen considering that the gradient should decrease by at least three orders of magnitude from the initial gradient [23]. The outer iteration cycle converges when the optimal value α of the objective function J is achieved

$$\alpha = \| [J]^{\beta} - [J]^{\beta-1} \| \leq \kappa \tag{26}$$

where β is the number of outer iterations. We have chosen $\kappa = 0.5$ for all the numerical experiments.

4.6 Computational Cost

The computational costs of the reduced model approach are dominated by the generation of the ensemble of forward model simulations. If the dynamics of the system does not change significantly during the coarse of simulation, then a smaller simulation period can be chosen for the generation of ensemble. Using this ensemble, the optimization problem can then be solved over the whole period of model simulation. The efficiency of the optimization process is also influenced by the ensemble size. A large ensemble size leads to a huge eigenvalue problem. It is possible to include only those snapshots in the ensemble where data are available.

The method needs to be updated in each outer iteration (β) by constructing a new POD model by generating a new ensemble of forward model simulations. The number of outer iterations β is influenced by the chosen abortion criterion κ. It should not be chosen too small because this causes jumping of objective function (J) because it is possible that the reduced model overestimates γ_k due to the process of linearization.

5. APPLICATION: DUTCH CONTINENTAL SHELF MODEL

The DCSM is an operational storm surge model, used in The Netherlands for real-time storm surge prediction in The North Sea. Accurate predictions of the storm surges are of vital importance to The Netherlands because large areas of the land lie below sea level. Accurate forecasts at least 6 h ahead are needed for proper closure of the movable storm surge barriers in Eastern Scheldt and the New Waterway. The governing equations used in DCSM are the nonlinear 2D shallow-water equations. The shallow-water equations, which describe large-scale water motions, are used to calculate the movements of the water in the area under consideration. These equations are

$$\begin{aligned} \frac{\partial u}{\partial t} + u\frac{\partial u}{\partial x} + v\frac{\partial u}{\partial y} + g\frac{\partial h}{\partial x} - fv + \frac{\rho_0 g u\sqrt{u^2+v^2}}{(D+h)C_{2D}^2} \\ = \frac{\tau_x}{D+h} - \frac{1}{\rho_w}\frac{\partial p_a}{\partial x} \end{aligned} \tag{27}$$

$$\frac{\partial v}{\partial t} + u\frac{\partial v}{\partial x} + v\frac{\partial v}{\partial y} + g\frac{\partial h}{\partial y} + fu + \frac{\rho_0 g v\sqrt{u^2+v^2}}{(D+h)C_{2D}^2} = \frac{\tau_y}{D+h} - \frac{1}{\rho_w}\frac{\partial p_a}{\partial y} \quad (28)$$

$$\frac{\partial h}{\partial t} + \frac{\partial [u(D+h)]}{\partial x} + \frac{\partial [v(D+h)]}{\partial y} = 0 \quad (29)$$

with

h = water level

u, v = depth-averaged current in x and y directions, respectively

D = water depth below the reference plane

f = Coriolis parameter

C_{2D} = 2D Chezy coefficient

τ_x, τ_y = wind stress in x and y directions, respectively

ρ_w = densty of water

p_a = atmospheric pressure

ρ_0 = background density

g = acceleration of gravity

These equations are descretized using an alternating directions implicit (ADI) method, and the staggered grid that is based on the method by [24] and improved by [25]. In the implementation, the spherical grid is used instead of rectangular (see, e.g., [26]). Boundary conditions are applied at both closed and open boundaries. At closed boundaries, the velocity normal to the boundary is zero. Thus, no inflow and outflow can occur through these boundaries. At the open boundaries, the water level is described in terms of ten harmonic components ($M_2, S_2, N_2, K_2, O_1, K_1, Q_1, P_1, U_2, L_2$) as follows:

$$h(t) = h_0 + \sum_{j=1}^{10} f_j H_j \cos(\omega_j t - \theta_j) \quad (30)$$

where

h_0 mean water level

H total water depth

$f_j H_j$ amplitude of harmonic constituent j

ω_j angular velocity of j

θ_j phase of j

The DCSM covers an area in the northeast European continental shelf (i.e., 12°W to 13°E and 48°N to 62°N), as shown in Fig. 1. The resolution of the spherical grid is $1/8^\circ \times 1/12^\circ$, which is approximately 8×8 km. With this configuration there are 201×173 grid with 19,809 computational grid points. The time step is $\triangle t$=10 min. All the open boundaries of the model are located in deep water (> 200 m) (see Fig. 1). This is done in order to model explicitely the nonlinearities of the surge tide interaction.

5.1 Estimation of Depth

The bathymetry for a model is usually derived from nautical maps. One of the purpose of these maps is to guide large ships safely through shallow waters. Therefore, these maps usually give details of shallow rather than deep-water areas. If we use these maps to prescribe the water depth, then it is reasonable to assume that this prescription of the bathymetry is erroneous. Thus depth can be a parameter on which model can be calibrated. In the early years of the developments of the DCSM, the changes to bathymetry were made manually. Later, automated calibration procedures based on variational methods were developed starting from the work by [1, 27]. The complete description on the development of these calibrated procedures for DCSM can be found in [28].

The experiments are performed to assimilate data near the Dutch coast [i.e., domain Ω (see Fig. 2)]. Obviously, not every depth point $D_{x,y}$ can be conceived as an unknown parameters of the simulation model. Including too many parameters, identifiability will become a problem [29]. The parameters groups should be selected in accordance with the physical properties of the model. It seems logical to avoid parameter groups in which the flow varies widely [4]. The numerical domain Ω is divided into subdomains $\Omega_k, k = 1, \ldots, 7$. These subdomains Ω_k are chosen based on uniformity of the depth in Ω_k. For each subdomain Ω_k, a correction parameter γ_k^b is defined that is related to $D_{x,y}$ by

$$D_{x,y} = D_{x,y}^M + \gamma_k^b; \quad \text{if} \quad (x,y) \in \Omega_k \quad (31)$$

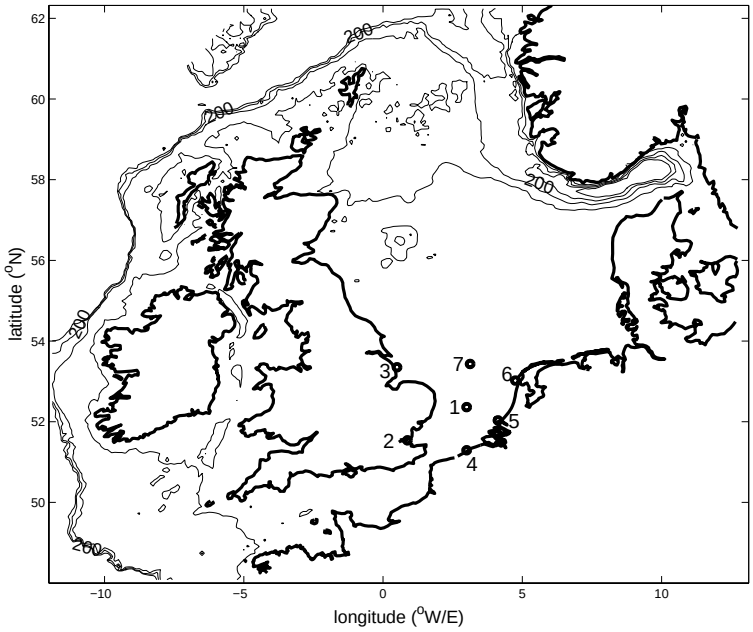

FIGURE 1. DCSM area and assimilation stations: 1. N51, 2. Southend, 3. Innerdowsing, 4. Oostende, 5. H.v.Holland, 6. Den Helder, 7. N4

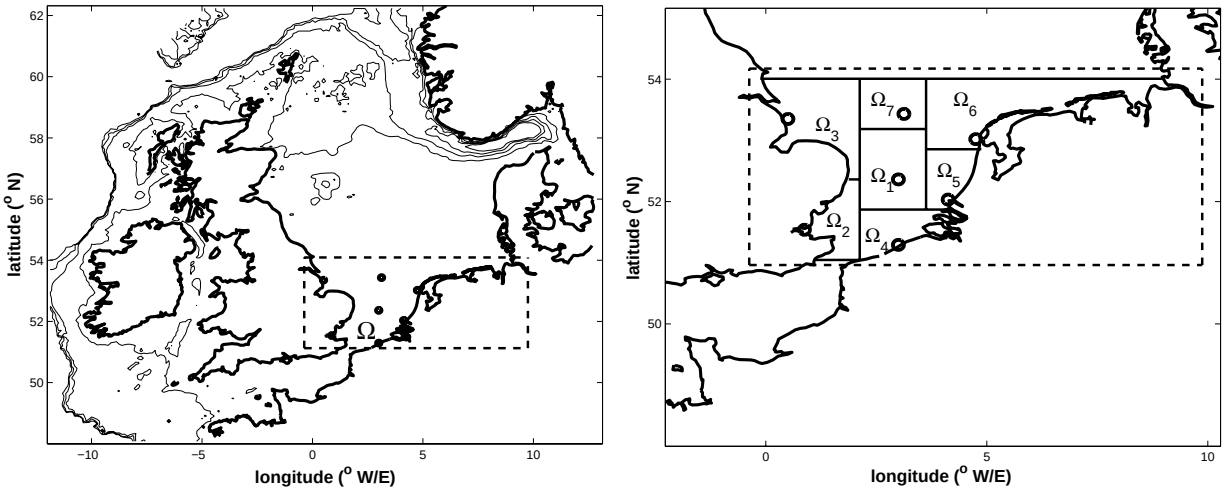

FIGURE 2. **(a)** Shows the domain Ω (dashed rectangle), of DCSM. **(b)** Shows the subdomains $\Omega 1$, $\Omega 2$, $\Omega 3$, $\Omega 4$, $\Omega 5$, $\Omega 6$ and $\Omega 7$

with $D^M_{x,y}$, the value used in the operational model. The parameters γ^b_k are treated as unknown parameters that are to be estimated. They act as a correction for the mean level of $D_{x,y}$ in a subdomain Ω_k and leave the spatial dependence inside Ω_k unaltered.

5.2 Experiment 1

Seven observation points are included in the assimilation, two of which are located along the east coast of the UK, two along the the Dutch coast, and one

at the Belgium coast (see Fig. 1). The truth model is run for a period of six days from December 13, 1997, 00:00, to December 18, 1997, 24:00, with the specification of water depth $D^M_{x,y}$ as used in the operational DCSM to generate artificial data at the assimilation stations. The first two days are used to properly initialize the simulations, and the set of observations $\mathbf{y}$ of computed water levels h are collected for last four days at an interval of every 10 min in seven selected assimilation grid points, which coincide with the points where data are observed in reality. We have assumed that the observations are perfect. This assumption is made in order to see how close the overestimate is with respect to the truth.

Then, 5[m] is added in $D^M_{x,y}$ at all the grid points in domain Ω to get the initial adjustments γ^b_k. With this specification of the background initial parameters γ^b_k, an ensemble E of 210 snapshot vectors are collected for the period where data are available i.e., from December 15, 1997, 00:00, to December 18, 1997, 24:00. The snapshots are chosen with an equal interval of 20 time steps; thus, 30 snapshots are collected for each estimate variable γ_k.

Each snapshot vector consists of predicted water levels h and velocities u and v. Therefore, it is necessary to scale the snapshot vectors before solving the eigenvalue problem (9). The state vector should be scaled such that all state variables become equally observable. For the shallow-water equations, the scaling based on energy produced at the output can be used to find a practical scaling method [30]. The potential and kinetic energies for one grid cell are

$$E_h = \frac{1}{2gh^2\rho_w \Delta x \Delta y} \tag{32}$$

$$E_{u,v} = \frac{1}{2(u^2+v^2)D\rho_w \Delta x \Delta y} \tag{33}$$

Assume one measures surface elevations. Through propagation of the model, kinetic energy may become potential energy and because the model is dissipative, the sum of the two can only decrease or at most remain the same. This suggests that scaling the state variables according to the energy they represent, creates approximately equal observability if the dissipation is small. In this case, the water levels h should be scaled with $\sqrt{g}$ and the velocities u and v with $\sqrt{D}$ [30].

After applying the above scaling to each snapshot vector in an ensemble E, we are able to form a basis consisting of only 15 dominant eigenmodes that captured 97% relative energy. Figure 3 shows POD modes captured energy for 210 snapshot vectors. Thus, a reduced model is built using these

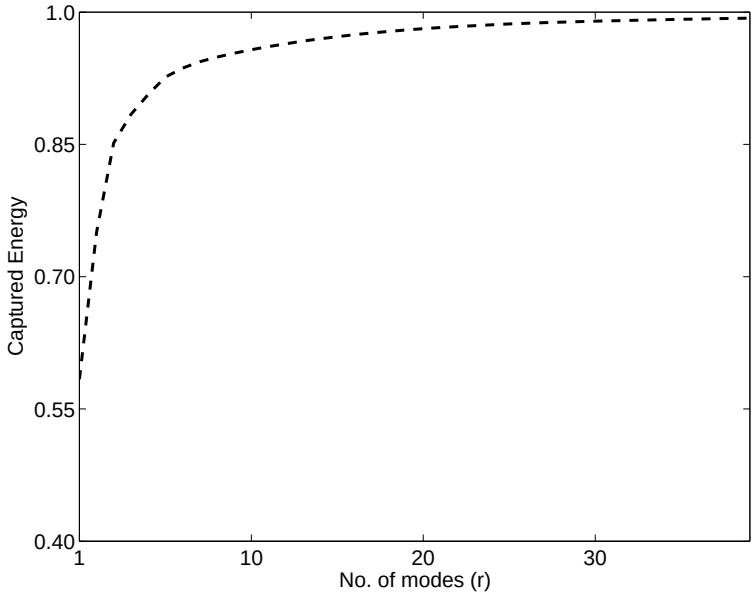

FIGURE 3. The POD modes capture energy for an ensemble of 210 snapshots of the water-level h(m), velocities u and v

15 modes and finally operates on dimension $\Re^{15+7}$. The low-dimensional model is defined by assuming that the matrix $\widetilde{M}$ remains stationary througout the experiment.

The numerical solution of the optimal control problem is obtained by the Quasi-Newton method with the LBFGS (limited memory Broyden Fletcher Goldfard Shanno) updating formula. With this reduced model, approximate objective function $\hat{J}$ is minimized and new values of estimate variables are found. The objective function J is reduced by $> 80\%$ after the inner minimization. We stopped the inner minimization process and switched to a new outer iteration with the new set of parameters following the criterion (μ), that the gradient should decrease by at least three order of magnitude from the initial gradient value. A new POD model is required in the outer iteration, if the old POD model cannot substantially reduces the objective function J. Figure 4 shows the history of the minimization of the objective function J in the POD-based estimation approach with respect to number of outer iterations (β). It is clear from Fig. 4 that after four outer iterations the objective function J is approximately equal to its optimal value.

In the beginning of the minimization process, there is a significant difference in parameters for regions that coincide with the UK, Dutch, and Belgish coast, but in the deep-water regions Ω_1 and Ω_7, there is not much improvement. The subdomains containing deep areas are less sensitive as compared to the subdomains containing shallow areas; thus, it is difficult to estimate γ_k^b in these areas. However, in the third and fourth outer iterations, we have found improvement in the deep-water regions Ω_1 and Ω_7. Figure 5 shows the convergence of parameters that coincide with coastal areas.

Figure 6 present three water levels at Den Helder and Hoek van Holland, respectively, for the period of December 16, 1997, 00:00, to December 18, 1997, 24:00. These time series refer to water levels obtained from simulated data (truth), forecast using deterministic model without data assimilation, and forecast with data assimilation after four outer iterations, respectively. These figures demonstrate that the differences between the forecasts with data assimilation and the truth are always smaller as compared to the difference between the forecasts without data assimilation and truth. It is also clear from the figures that both the effects, phase shift and correct amplitude, are compensated.

To quantify the performance of the POD-based estimation method at assimilation stations, we use root-mean-square (rms) metric of the water-level errors over the whole simulation period

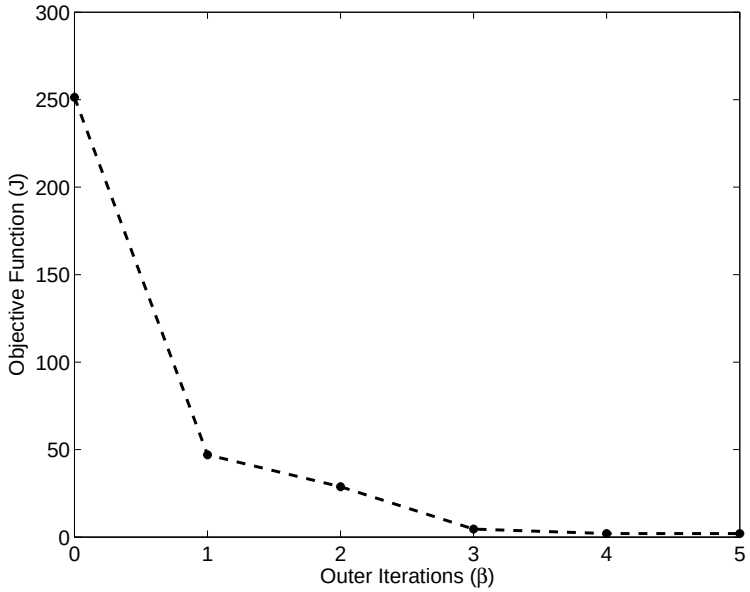

FIGURE 4. Graph of the objective function (J) versus the number of outer iterations (β)

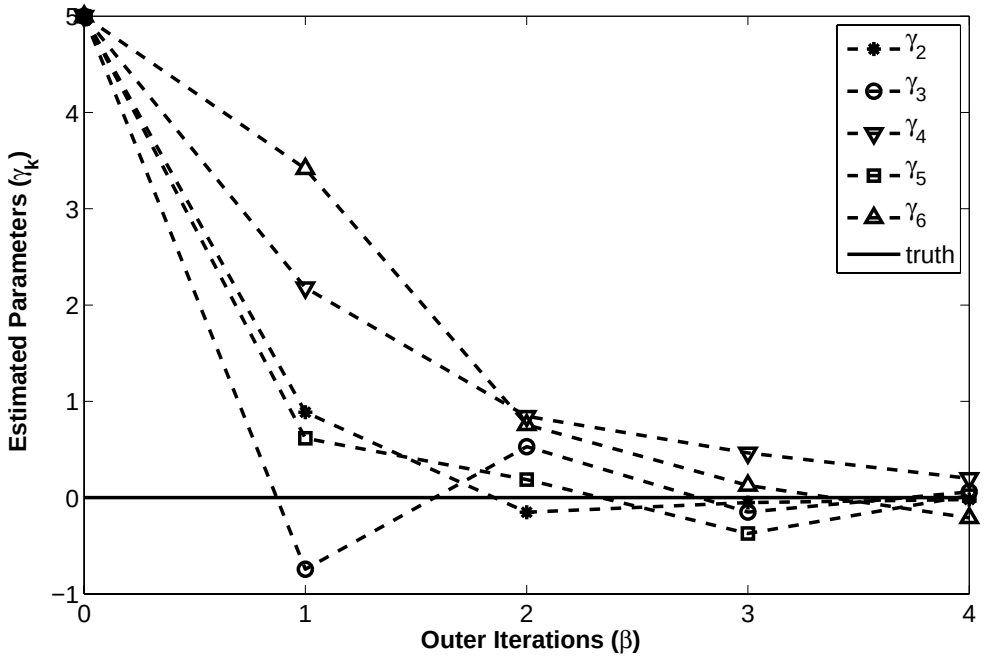

FIGURE 5. Convergance of the depth parameters that coincide along UK, Dutch and Belgium coasts

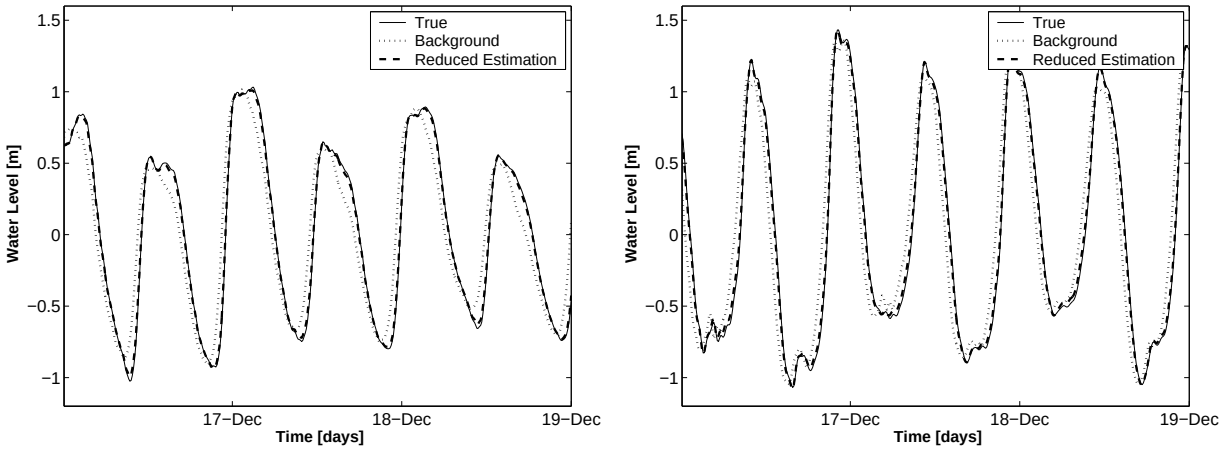

(a) (b)

FIGURE 6. Water level timeseries for the period from December 16, 1997, 00:00, to December 18, 1997, 24:00. simulated data (truth), deterministic model without assimilation (background), forecasts with data assimilation after four outer iterations (reduced estimation) at **a)** Den Helder **b)** Hoek van Holland

$$\text{rms} = \sqrt{\frac{1}{m}\sum_{i=1}^{m}\left[\zeta^t(t_i) - \hat{\zeta}(t_i)\right]^2} \tag{34}$$

with ζ^t is the water level at truth and $\hat{\zeta}$ is the analyzed water level. To check whether the data assimilation works also at other locations, the rms water-level innovations are also computed in some validation stations, where no assimilation was performed. We have in our experiments, six validation stations. Figure 7 shows rms water-level innovation at the assimilation and validation stations, respectively. The POD-based estimation procedure reduces the rms values of the water-level errors at both the assimilation and validation stations.

In order to get an idea of the required computational cost, we express it in terms of number of simulations with the original model. In this experiment, seven parameters are estimated; thus, eight model simulations for a period of six days are performed to generate an ensemble. The snapshots are collected for only the last four days, because observations are available for this period. Because only 210 snapshots are chosen, the computational time to

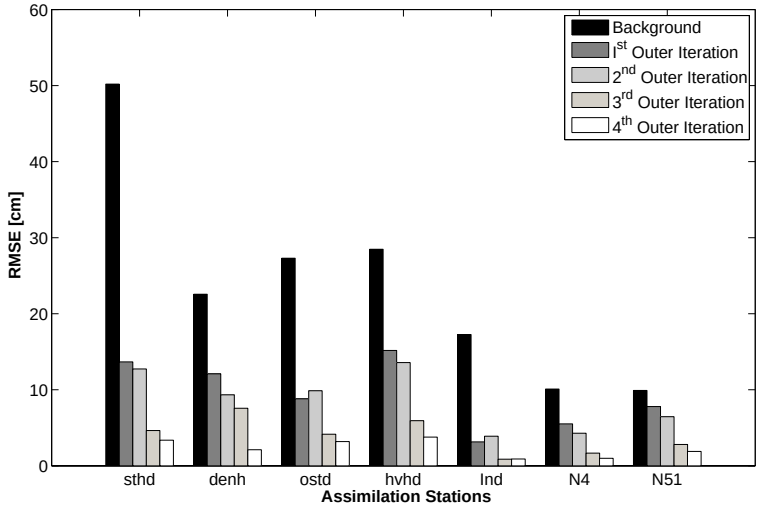

(a)

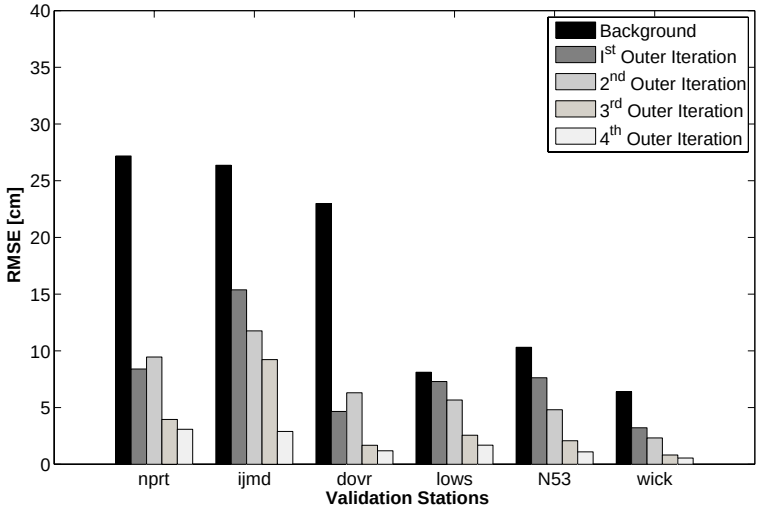

(b)

FIGURE 7. RMS errors with respect to water level observations at **a)** assimilation stations and **b)** validation stations

solve the eigenvalue problem and to construct the reduced model is much less than that of running the full model. Combined with seven estimate variables, the reduced model operated eventually in R^{22} instead of $\sim 6 \times R^{10^4}$. To simulate the POD reduced model and its adjoint model over the whole simulation period requires approximately $1/50$ of the full model. The number of outer iterations (β) in the experiment are four. Therefore, the time required to estimate seven parameters with the POD-based reduced estimation procedure is equal to ~ 34 simulations with the original model. The same amount of time is required in the case of the classical adjoint method (see [31]). Thus, the POD calibration method offers an efficiency comparable to the classical adjoint method, without the burden of implementation of the adjoint.

5.3 Experiment 2

In this experiment, we have computed POD reduced model from a short simulation and used it for a calibration on a longer period. For the same specification of a boundary forcing and the water depth $D^M_{x,y}$, as for previous experiment, a truth model is run for 15 days (i.e., from December 13, 1997, 00:00, to December 27, 1997, 24:00), to generate artificial data (observations) for last 13 days. These observations $\mathbf{y}$ are again the computed water levels for the same assimilation stations.

The specification of the background initial parameters γ^b_k is the same as in the previous experiment. We used the same POD reduced-order model, which was constructed from an ensemble E of 210 snapshot vectors of forward model simulations for the period from December 13, 1997, 00:00, to December 18, 1997, 24:00 (six days), as in the previous experiment. The calibration period is now 15 days (i.e., December 13, 1997, 00:00, to December 27, 1997, 24:00).

The approximate objective function $\hat{J}$ reduces the cost with similar magnitude. Figure 8 shows the minimization of the objective function J in the experiment with respect to the number of outer iterations. The existence of the same trend in this graph as compared to the minimization of objective function J in calibration over six days indicates that the POD reduced model constructed over the small time period can be used for calibration over a much larger period.

Figure 9 shows rms errors of water level at the assimilation stations. The estimation procedure reduces the rms values of the water level errors at all the assimilation stations. Figure 10 gives an indication of the model performance after calibration and presents the water-level time series at Hoek van

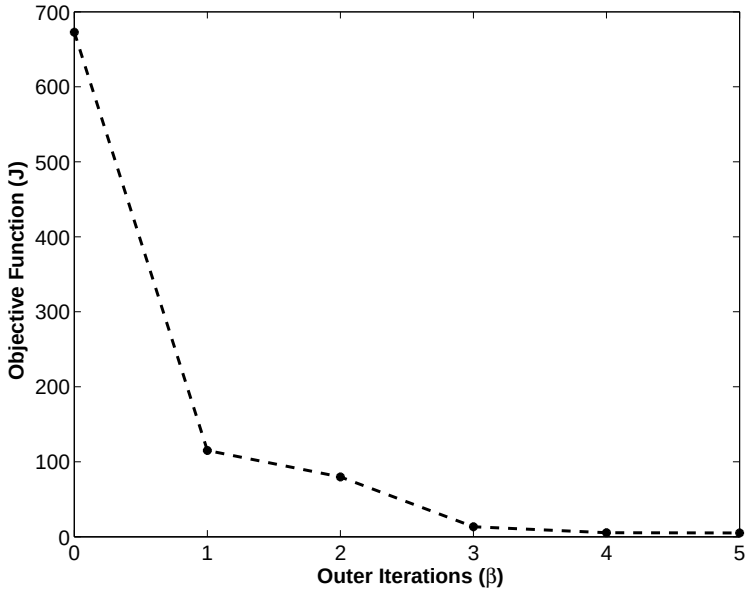

FIGURE 8. Graph of the objective function (J) versus the number of outer iterations (β), for the calibration over 15 days

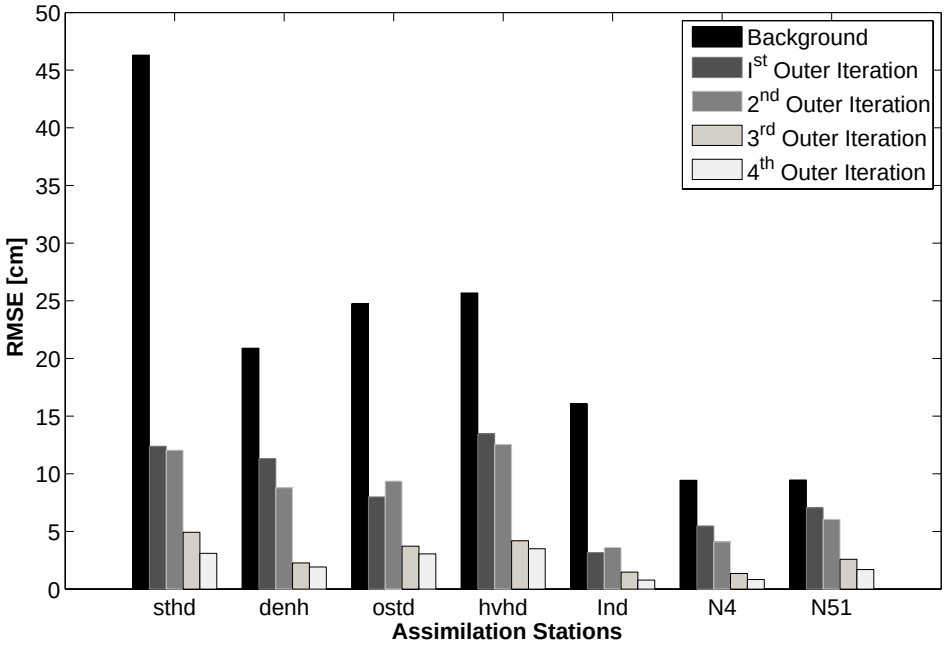

FIGURE 9. RMS errors with respect to water level observations at assimilation stations for calibration over 15 days

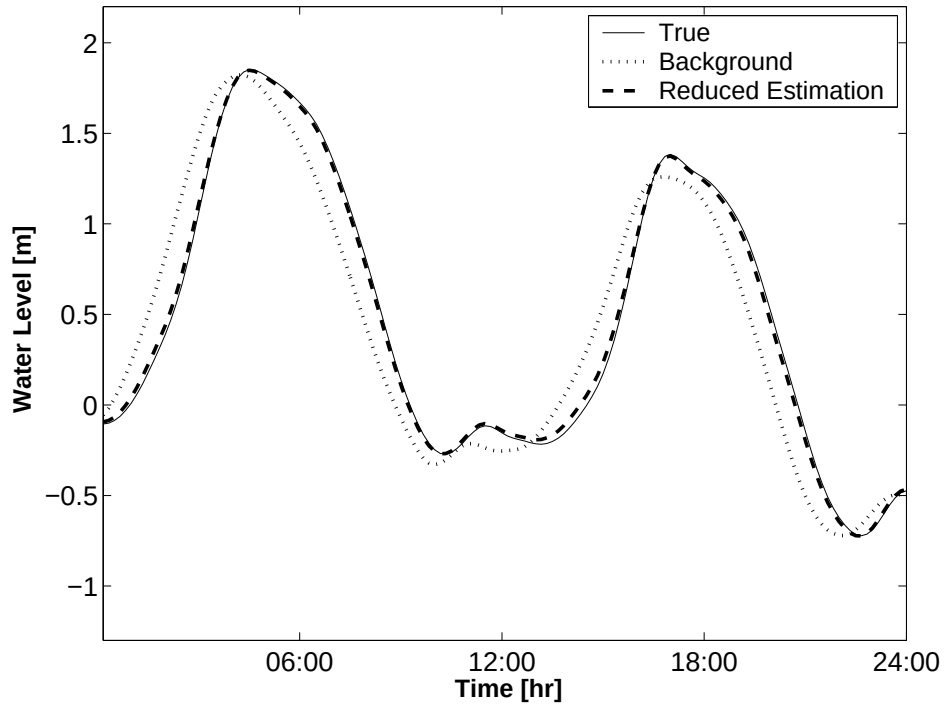

FIGURE 10. Water level timeseries at Hoek van Holland for the period from December 24, 1997, 00:00, to December 24, 1997, 24:00. for simulated data (truth), the initial setting of the calibration parameters (background) and forecasts with data assimilation after four outer iterations (reduced estimation)

Holland for the period of December 24, 1997, 00:00, to December 24, 1997, 24:00, for the initial setting of the calibration parameters, the true calibration parameters, and the calibration parameters after four outer iterations with the reduced estimation procedure.

In this experiment, seven parameters are estimated for a calibration over 15 days. Seven model simulations for a period of six days and one model simulation with background initial parameters for a period of 15 days are performed to generate an ensemble. The total number of outer iterations (β) in the experiment are four; therefore, the time required to estimate seven parameters is now $\sim$ 17 simulations with the original model. Thus, for the current experiment, POD reduced model required $1/2$ of the computational time of the classical adjoint method. The experiment significantly reduces the computational cost.

6. CONCLUSION

The adjoint method is a powerful tool for sensitivity analysis and model calibration, but it is laborious to implement an adjoint model for the computation of the gradient for large-scale systems. The model-reduction approach presented here is used to simplify this problem using a projection-based POD model reduction method. An optimal order-reduction approach to model calibration must accurately capture the properties of the full dynamical model. The present approach is designed to approximate the data assimilation system in a restricted space while retaining its essential properties. We have shown that the method fits into the theory of incremental variational data assimilation by using restriction and prolongation operators.

The method has been used to calibrate the operational model for storm surge prediction, the two-dimensional DCSM. Twin experiments have been performed to estimate the water depth. The results show that the calibration method performs very efficiently. A POD reduced model of such a small size (R^{15}) has been constructed instead of original model of size ($\sim 6 \times R^{10^4}$). After four outer iterations (β), the objective function (J) has been reduced significantly and is very close to optimal value. The rms errors at both assimilation and validation stations have improved significantly.

Considering the periodicity in the model with respect to time, an experiment has been done to calibrate the model for a longer period with a reduced-order model over the shorter period. The same trend in the minimization of objective function (J) has been observed for the calibration over 15 days, from the same POD model that is used for the calibration over six days. This result demonstrates the potential use of the method to calibrate DCSM model for a much longer period. Moreover, the POD calibration method offers a relatively efficient method compared to the classical adjoint method, without the burden of implementation of the adjoint.

The classical method gives the adjoint of the tangent linear model, which is replaced here by the adjoint of the linear reduced model. Compared to the classical adjoint method, the minimization in reduced space converges faster due to a better condition number of the reduced Hessian. The method has a limitation that it has to be updated in each outer loop by constructing a new POD model by generating an ensemble of forward model simulations. More efforts are required to obtain a reduced-order methodology that fits in the framework of data assimilation. Especially, the quality of ensemble and the process of generating ensemble are crucial for a reduced-order procedure to be effective. The preliminary results of the experiments on the use of POD method to calibrate DCSM are encouraging. Here, we have used simulated data and the number of parameters estimated are small. The next step in our future research is to use the POD method to calibrate DCSM with real data.

ACKNOWLEDGMENTS

We thank Nils van Velzen of VORtech for support with the COSTA software [32]. COSTA is an open-source project that provides a free toolbox for data assimilation.

APPENDIX A

Equation (23) introduces the adjoint model $\hat{\mathbf{v}}(t_{i+1})$, that is elaborated here. The approximate objective function $\hat{J}$ can be written as

$$\hat{J}(\Delta\gamma) = \sum_{i=1}^{m} \Big(\hat{H}^T \left\{ \mathbf{y}(t_i) - H\left[\mathbf{x}^b(t_i)\right] \right\} - \xi(t_i, \Delta\gamma) \Big)^T P^T R_i^{-1} P \Big(\hat{H}^T \left\{ \mathbf{y}(t_i) - H\left[\mathbf{x}^b(t_i)\right] \right\} - \xi(t_i, \Delta\gamma) \Big) \tag{A1}$$

The reduced adjoint state variables $\hat{\mathbf{v}}$ are introduced in Eq. (A1) as

$$\hat{J}(\Delta\gamma) = \bar{J}(\Delta\gamma) + \sum_{i=1}^{m} \hat{\mathbf{v}}(t_{i+1})^T \times \left[\xi(t_{i+1}, \Delta\gamma) - A_i \xi(t_i, \Delta\gamma) \right] \tag{A2}$$

where $\hat{J} \equiv \bar{J}$. The matrix A_i is defined as

$$A_i = \begin{pmatrix} \widetilde{M}_i & \widetilde{M}_i^{\gamma} \\ 0 & I \end{pmatrix} \tag{A3}$$

The incremental changes in $\hat{J}$, $\xi(t_i, \Delta\gamma)$ and $\hat{\mathbf{v}}$ due to incremental change in one of the components of $\Delta\gamma$ gives

$$\begin{aligned} \Delta\hat{J} = & \sum_{i=0}^{m-1} \hat{\mathbf{v}}(t_{i+1})^T \left[\Delta\xi(t_{i+1}, \Delta\gamma) - A_i \Delta\xi(t_i, \Delta\gamma) \right] + \textstyle\sum_{i=0}^{m-1} \Delta\hat{\mathbf{v}}(t_{i+1})^T \\ & \times \left[\xi(t_{i+1}, \Delta\gamma) - A_i \xi(t_i, \Delta\gamma) \right] \\ & - \sum_{i=0}^{m-1} \hat{\mathbf{v}}(t_{i+1})^T \frac{\partial \xi(t_{i+1}, \Delta\gamma)}{\partial \Delta\gamma} \Delta\gamma \\ & + \left[\frac{\partial J}{\partial \xi(t_i, \Delta\gamma)} \right]^T \Delta\xi(t_i, \Delta\gamma) \end{aligned} \tag{A4}$$

The above expression after simple calculations yields:

$$\begin{aligned} \Delta\hat{J} = & \sum_{i=1}^{m-1} \Delta\xi(t_i, \Delta\gamma) \left[\hat{\mathbf{v}}(t_i)^T - A_i \hat{\mathbf{v}}(t_{i+1})^T \right] \\ & + \left[\frac{\partial J}{\partial \xi(t_i, \Delta\gamma)} \right]^T \Delta\xi(t_i, \Delta\gamma) \\ & + \hat{\mathbf{v}}(t_m)^T \Delta\xi(t_m, \Delta\gamma) - \sum_{i=0}^{m-1} \hat{\mathbf{v}}(t_{i+1})^T \\ & \times \frac{\partial \xi(t_{i+1})}{\partial \Delta\gamma} \Delta\gamma \end{aligned} \tag{A5}$$

An expression for the reduced adjoint model $\hat{\mathbf{v}}(t_{i+1})$; $i \in \{m-1, \cdots, 1\}$ solved backward in time is followed from above expression:

$$\hat{\mathbf{v}}(t_i) = A_i^T \hat{\mathbf{v}}(t_{i+1}) + B(t_i) \tag{A6}$$

with $\hat{\mathbf{v}}(t_m)$ equals zero. $B(t_i)$ is given by:

$$B(t_i) = \begin{pmatrix} -2P^T R_i^{-1} P \Big[\hat{H}^T \left\{ \mathbf{y}(t_i) - H\left[\mathbf{x}^b(t_i)\right] \right\} - \xi(t_i, \Delta\gamma) \Big] \\ \\ 0 \end{pmatrix}$$

Once the reduced adjoint states $\hat{\mathbf{v}}(t_i)$ are known, the gradient $\partial\hat{J}/\partial\Delta\gamma$ is found as:

$$\frac{\Delta\hat{J}}{\Delta\gamma} = \sum_i -[\hat{\mathbf{v}}(t_{i+1})]^T \frac{\partial \xi(t_{i+1})}{\partial \Delta\gamma} \tag{A7}$$

REFERENCES

1. Ten-Brummelhuis, P. G. J., Heemink, A. W., and van den Boogard, H. F. P., Identification of shallow sea models. *Int. J. Numer. Methods Fluids.* **17**:637-665, 1993.
2. Lardner, R. W., Al-Rabeh, A. H., and Gunay, N., Optimal Estimation of Parameters for a Two Dimensional Hydrodynamical Model of the Arabian Gulf. *J. Geophys. Res. Oceans.* **98**:229-242, 1993.
3. Ulman, D. S., and Wilson, R. E., Model Parameter Estimation for Data Assimilation Modeling: Temporal and Spatial Variability of the Bottom Drag Coefficient. *J. Geophys. Res. Oceans.* **103**:5531-5549, 1998.
4. Heemink, A. W., Mouthaan, E. E. A., and Roest, M. R. T., Inverse 3D Shallow-Water Flow Modeling of the Continental Shelf. *Continental Shelf Research*. **22**:465-484, 2002.
5. Kaminski, T., Giering, R., and Scholze, M., An Example of an Automatic Differentiationbased Modeling System. *Lecture Notes Comput. Sci.* **2668**:5-104, 2003.
6. Antoulas, A. C., *Approximation of Large-Scale Dynamical Systems*. Philadelphia, PA: SIAM, 2005.
7. Pearson, K., On Lines and Planes of Closest Fit to Points in Space. *Phil. Mag.* **2**(6):559-572, 1901.
8. Kepler, G. M., Tran, H. T., and Banks, H. T., Reduced-Order Compensator Control of Species Transport in CVD Reactor. *Optim. Control Appl. Methods.* **21**(4):143-160, 2000.

9. Prabhu, R. D., Scott, C. S., and Changly, Y., The Influence of Control on Proper Orthogonal Decomposition of Wall-Bounded Turbulent Flows. *Phys. Fluids*. **13**:229-242, 2001.
10. Alfonsi, G., Restanob, C., and Primaveral, L., Coherent Structures of the Flow around a Surface-Mounted Cubic Obstacle in Turbulent Channel Flow. *J. Wind Eng. Ind. Aerodyn*. **91**:495-511, 2003.
11. Cao, Y., Zhu, J., Luo, Z., and Navon, I. M., Reduced Order Modeling of the Upper Tropical Pacific Ocean Model Using Proper Orthogonal Decomposition. *Comput. Math. Appl.* **52**:1373-1386, 2006.
12. Gunzburger, M. D., Reduced-Order Modeling, Data Compression and the Design of Experiments. In Second DOE Workshop on Multiscale Mathematics, Broomfield, CO, 2004.
13. Le Dimet, F. X., and Talagrand, O., Variational Algorithms for Analysis and Assimilation of Meteorological Observations: Theoratical Aspects. *Tellus*. **38**:97-110, 1986.
14. Lawless, A. S., Nichols, N. C., Boess, C., and Bunse-Gerstner, A., Using Model Reduction Methods within Incremental 4DVAR. *Mon. Weather Rev.* **136**:1511-1522, 2008.
15. Daescu, D. N., and Navon, I. M., A Dual Weighted Approach to Order Reduction in 4DVAR Data Assimilation. *Mon. Weather Rev.* **136**:1026-1041, 2008.
16. Fang, F., Pain, C. C., Navon, I. M., Piggott, D., Gorman, G. J., Farrell, P. E., Allison, P. A., and Goddard, A. J. H., Reduced order modeling of an adaptive mesh ocean model. *Int. J. Numer. Meth. Fluids.*, **59**(8):827–851, 2009.
17. Fang, F., Pain, C. C., Navon, I. M., Piggott, D., Gorman, G. J., Allison, P. A., and Goddard, A. J. H., A POD Reduced-Order Unstructured Mesh Ocean Modelling Method for Moderate Reynolds Number Flows. *Ocean Model.* **28**:127-136, 2009.
18. Delay, F., Buoro, A., and de Marsily, G., Empirical Orthogonal Functions Analysis Applied to the Inverse Problem in Hydrogeology: Evaluation of Uncertainty and Simulation of New Solutions. *Math. Geology.* **33**:927-949, 2001.
19. Vermeulen, P. T. M., Heemink, A. W., and Valstar, J. R., Inverse Modeling of Groundwater Flow Using Model Reduction. *Water Resourc. Res.* **41**(6):1–13, 2005.
20. Vermeulen, P. T. M., and Heemink, A. W., Model-Reduced Variational Data Assimilation. *Mon. Weather. Rev.* **134**:2888-2899, 2006.
21. Courant, R., and Hilbert, D., *Methods of Mathematical Physics*. New York: Wiley Interscience, 1953.
22. Sirovich, L., Choatic Dynamics of Coherent Structures. *Physica D*. **37**:126-145, 1987.
23. Cao, Y., Zhu, J., Navon, I. M., and Luo, Z., A Reduced-Order Approach to Fourdimensional Variational Data Assimilation Using Proper Orthogonal Decomposition. *Int. J. Numer. Meth. Fluids*. **53**:1571-1583, 2007.
24. Leendertse, J., Aspects of a Computational Model for Long-Period Water Wave Propagation. Ph.D. Thesis, Rand Corp., Memo No. RM-5294-PR, Santa Monica, 1967.
25. Stelling, G. S., On the Construction of Computational Methods for Shallow Water Flow Problem. Ph.D. thesis, Rijkswaterstaat Communications 35, Rijkswaterstaat, 1984.
26. Verboom, G. K., de Ronde, J. G., and van Dijk, R. P., A Fine Grid Tidal Flow and Storm Surge Model of the North Sea. *Continental Shelf Res.* **12**:213-233, 1992.
27. Mouthaan, E., Heemink, A. W., and Robaczewska, K., Assimilation of ERS-1 Altimeter Data in a Tidal Model of the Continental Shelf. *Deuts. Hydrograph. Zeits.* **36**(4):285-319, 1994.
28. Verlaan, M., Zijderveld, A., Vries, H., and Kroos, J., Operational Storm Surge Forcasting in the Netherlands: Developments in Last Decade. *Phil. Trans. R. Soc. A*. **363**:1441-1453, 2005.
29. Verlaan, M., Mouthaan, E., Kuijper, E., and Philippart, M., Parameter Estimation Tools for Shallow Water Flow Models. *Hydroinformatis.* **96**:341-348, 1996.
30. Verlaan, M., Efficient Kalman Filtering Algorithms for Hydrodynamic Models. Ph.D. thesis, Technical University Delft, The Netherlands, 1998.

31. Ten-Brummelhuis, P. G. J., Parameter Estimation in Tidal Flow Models with Uncertain Boundary Conditions. Ph.D. thesis, Twente University, The Netherlands, 1992.

32. Velzen, N., and Verlaan, M., Costa a Problem Solving Environment for Data Assimilation Applied for Hydrodynamical Modeling. *Meteorolog. Zeits.* **16**:777-793, 2007.